APPLIED PHYSICS LETTERS **87**, 121903 (2005)

Thermal annealing effect on the band gap and dielectric functions of silicon nanocrystals embedded in SiO_2 matrix

L. Ding, T. P. Chen,[a] Y. Liu, and C. Y. Ng
School of Electrical and Electronic Engineering, Nanyang Technological University, Singapore 639798

Y. C. Liu
Singapore Institute of Manufacturing Technology, Singapore 638075

S. Fung
Department of Physics, The University of Hong Kong, Hong Kong

(Received 18 April 2005; accepted 28 July 2005; published online 12 September 2005)

The thermal annealing effect on band gap and dielectric functions of silicon nanocrystals (*nc*-Si) embedded in a SiO_2 matrix synthesized by Si ion implantation is investigated by spectroscopic ellipsometry. A large band-gap expansion of *nc*-Si relative to bulk crystalline silicon has been observed. The band gap of the *nc*-Si for the nonannealing condition (i.e., as implanted) is 1.78 eV while it is 1.72 eV for the annealing at 1000 °C for 100 min. The slight decrease in the band gap is attributed to the slight increase in the *nc*-Si size with annealing. The dielectric functions of *nc*-Si show a significant suppression, as compared to bulk crystalline silicon, due to the quantum size effect. Annealing results in a small change in the static dielectric constant, which can be explained in terms of the size effect also. © *2005 American Institute of Physics*.
[DOI: 10.1063/1.2051807]

There has been an increasing interest in semiconductor nanostructures after the initial work of Canham on visible luminescence from porous silicon,[1] because of their light-emission ability with high efficiency for potential applications in silicon-based optoelectronic devices. However, the practical application in optoelectronic devices of porous silicon is limited by its instability in light emission,[2] structural fragility, and incompatibility with conventional integrated circuit technology.[3] Therefore, silicon nanocrystals (*nc*-Si) are considered to be the preferable strategy for overcoming these challenges. Among the different techniques used to synthesize *nc*-Si, ion implantation of silicon into a dielectric matrix, preferably SiO_2 films, followed by high-temperature annealing, is deemed one of the most promising candidates for producing electrically and chemically stable silicon nanocrystals. This technique offers the advantage of being fully compatible with the complimentary metal-oxide-semiconductor (CMOS) process. In spite of the fact that efficient photoluminescence (PL) (Refs. 3–5) and electroluminescence (EL) (Refs. 6–8) in Si nanocrystals embedded in a SiO_2 matrix have been demonstrated, it remains necessary to accurately determine the dielectric functions of embedded *nc*-Si in order to perform reliable device modeling.

Many investigations on the optical properties of *nc*-Si have been carried out by luminescence studies[3–8] and theoretical calculations.[9–13] However, very few studies focused on the optical properties of *nc*-Si embedded in SiO_2 being prepared with Si ion implantation under different annealing conditions. In this work, we present a comprehensive optical study on *nc*-Si embedded in a SiO_2 matrix with spectroscopic ellipsometry (SE) in the photon-energy range of 1.1–5 eV. A multilayer optical model that takes into account the distribution of implanted Si ions is designed to analyze the SE response [i.e., $\tan(\psi)$ and $\cos(\Delta)$ where ψ and Δ are the ellipsometric angles]. The Maxwell-Garnett effective-medium approximation (EMA) combined with the four-term Forouhi-Bloomer (FB) (Ref. 14) model has been used to determine the dielectric functions of *nc*-Si embedded in the SiO_2 matrix synthesized with different annealing times. A large optical band-gap expansion and a strong dielectric suppression for *nc*-Si have been observed from the analysis based on the FB model. The effects of postimplantation thermal annealing on both the band gap and the dielectric functions of the *nc*-Si have been investigated.

550-nm-thick SiO_2 thin films were grown on *p*-type silicon substrates with (100) orientation by thermal oxidation in dry oxygen at 950 °C. A dose of 1×17 atoms/cm^2 Si ions were then implanted into SiO_2 films at the energy of 100 keV. Postimplantation thermal annealing was carried out in nitrogen ambient at various temperatures for different annealing times. For simplicity, only the results of annealing at 1000 °C for various annealing durations ranging from 0 to 100 min (0, 20, 30, 40, 60, 80, and 100 min) are presented here. The average size of *nc*-Si was determined from the broadening of the Bragg peak in x-ray diffraction (XRD) measurements.[15] The *nc*-Si size obtained was from ~3.3 nm for the as-implanted sample to ~4.5 nm for the samples annealed at 1000 °C for different durations. The *nc*-Si sizes for various annealing durations obtained from the XRD measurements are shown in Table I. A very small increase in the *nc*-Si size with annealing is observed. This slow evolution in the size is due to the very low diffusion coefficient of Si in the SiO_2 film, being consistent with the results reported in Ref. 16. The SE measurements were carried out in the wavelength range of 250 and 1100 nm with a step of 5 nm, and the incidence angle was set to 75°.

The profile of excess Si in the SiO_2 thin films was measured with secondary-ion mass spectroscopy (SIMS). The implanted Si distributes from the surface to the depth of ~250 nm, and the subsequent annealing does not change the profile significantly because of the extremely low diffusion coefficient of Si in SiO_2 films. There is almost no *nc*-Si beyond the depth of 250 nm in the SiO_2 film. In order to

[a]Electronic mail: echentp@ntu.edu.sg

 © 2005 American Institute of Physics
Downloaded 19 Apr 2007 to 147.8.143.135. Redistribution subject to AIP license or copyright, see http://apl.aip.org/apl/copyright.jsp

TABLE I. Size, band gap, and static dielectric constant of *nc*-Si annealed for different durations. E_g^{exp} and $\varepsilon_{static}^{exp}$ are the band gap and the static dielectric constant of *nc*-Si obtained from the spectral fittings based on the four-term FB model, respectively. E_g^{cal} is the *nc*-Si band gap obtained from the calculation with Eq. (1), while $\varepsilon_{static}^{cal}$ is the *nc*-Si static dielectric constant obtained from the calculation with Eq. (2).

Annealing time (min)	Size (nm)	E_g^{cal} (eV)	E_g^{exp} (eV)	$\varepsilon_{static}^{cal}$	$\varepsilon_{static}^{exp}$
0	3.3±0.4	2.03±0.15	1.78	8.98±0.34	8.82
20	4.6±0.2	1.73±0.03	1.74	9.72±0.08	9.67
30	4.2±0.2	1.79±0.05	1.74	9.54±0.10	9.52
40	4.5±0.2	1.74±0.04	1.74	9.68±0.09	9.73
60	4.3±0.2	1.78±0.04	1.75	9.59±0.10	9.73
80	4.5±0.2	1.74±0.04	1.74	9.68±0.10	9.61
100	4.5±0.2	1.74±0.04	1.72	9.68±0.10	9.73

extract the dielectric functions of *nc*-Si embedded in SiO_2, the multilayer optical model shown in Fig. 1 was used to analyze the SE data. As can be seen in Fig. 1, the layer containing *nc*-Si, whose thickness d_1 is 250 nm, is divided into 25 sublayers with equal thickness d_0=10 nm. Each sublayer can be optically schematized as an effective medium represented by the Maxwell-Garnett EMA. The Maxwell-Garnett EMA is characterized by the volume fraction of *nc*-Si which can be obtained from the SIMS measurement, the known dielectric functions of SiO_2, and the *nc*-Si dielectric functions that are to be determined. Therefore, the Maxwell-Garnett EMA is used to extract the *nc*-Si dielectric functions from the SE spectral fitting. For the spectral fitting an optical dispersion model for the *nc*-Si is required. We have found that the four-term FB model[14] is the suitable one that can yield a successful fitting. As such, the Maxwell-Garnett EMA based on the four-term FB model is used in the SE spectral fitting. In the spectral fitting, the optimization is carried out by freely varying the 14 parameters,[14] which include the parameters A_i, B_i, C_i (i=1, 2, 3, and 4) for the four terms, the refractive index $n(\infty)$ when photon energy $E \rightarrow \infty$, and the band gap E_g to minimize the mean-square error (MSE) (Ref. 17). As a typical example, the spectral fitting of the sample annealed for 30 min, which has a MSE of 0.012, is shown in Fig. 2. A very small MSE (0.007–0.019) is also obtained for other samples. The excellent spectral fittings of all samples indicate that the four-term FB dispersion relation can accurately describe the spectral dependence of the *nc*-Si dielectric functions.

The *nc*-Si band gap (E_g) obtained from the spectral fittings for various annealing durations is given in Table I. The *nc*-Si shows a large expansion in the band gap as compared to the bulk crystalline silicon, i.e., a band-gap expansion of ~0.6 eV is observed. The *nc*-Si band gap obtained in this work is in very good agreement with the first-principles calculation of the optical gap of silicon nanocrystals based on quantum confinement.[11] A fit to the calculation shown in Fig. 3 of Ref. 11 yields

$$E_g(D) = E_{g0} + C/D^n, \tag{1}$$

where D is the nanocrystal size in nm, $E_g(D)$ is the band gap in eV of the nanocrystal, E_{g0}=1.12 eV is the band gap of bulk crystalline Si, C=3.9, and n=1.22. For comparison, the band gap of *nc*-Si calculated with Eq. (1) is presented in Table I. The very good agreement shown in Table I strongly suggests that the band-gap expansion is a result of quantum size effect.

As examples, the dielectric functions of *nc*-Si obtained after 0 (nonannealing), 30, and 80 min of annealing are shown in Fig. 3. The dielectric functions of bulk crystalline silicon are also included in the figure for comparison. Obviously, the *nc*-Si exhibits a significant reduction in the dielectric functions with respect to bulk crystalline silicon. It is observed that the dielectric-function spectra of the *nc*-Si of

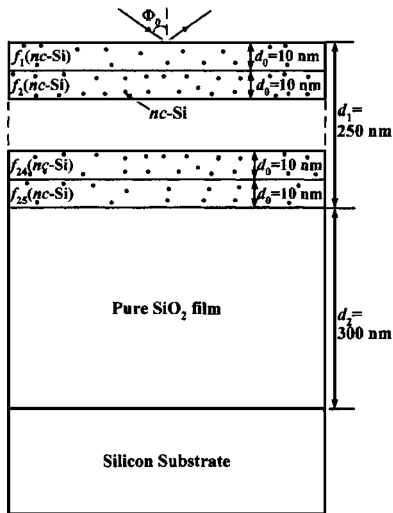

FIG. 1. Multilayer model used in the SE analysis. The thickness of the SiO_2 thin film grown on the silicon substrate is 550 nm, the *nc*-Si distributes from the surface to the depth (d_1) of 250 nm in the SiO_2 film, and thus the thickness (d_2) of the pure SiO_2 layer is 300 nm. The *nc*-Si-distributed layer with the thickness d_1 is divided into 25 sublayers with equal thickness d_0 =10 nm. The volume fraction of the *nc*-Si in each sublayer is f_i(*nc*-Si) (i =1,2,...,25). The diagram is not drawn to scale.

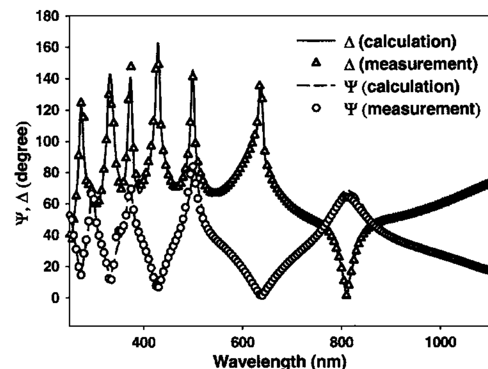

FIG. 2. Typical spectral fitting of the ellipsometric angles ψ and Δ. The sample is annealed at 1000 °C for 30 min.

Downloaded 19 Apr 2007 to 147.8.143.135. Redistribution subject to AIP license or copyright, see http://apl.aip.org/apl/copyright.jsp

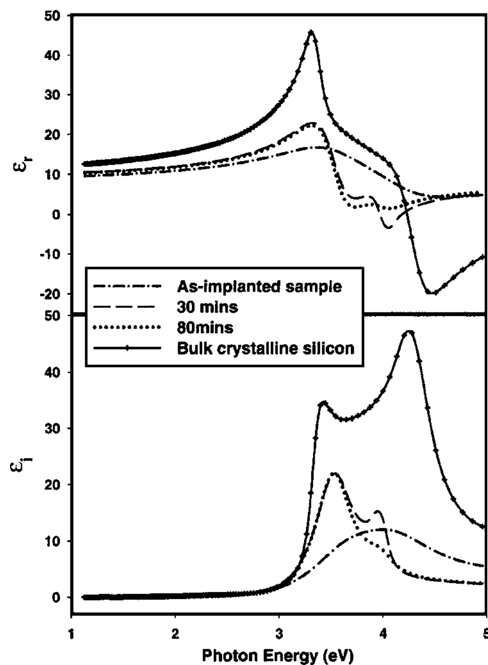

FIG. 3. Real (ε_r) and imaginary (ε_i) parts of the complex dielectric functions of both the *nc*-Si annealed for 0, 30, and 80 min and the bulk crystalline silicon as functions of photon energy.

different annealing durations, except the nonannealing sample, are very similar. This is not surprising, and it can be explained in terms of quantum size effect on the dielectric functions.[9,15] As shown in Table I, except for the nonannealing sample which shows a *nc*-Si size of ~3.3 nm, all other samples with different annealing durations have almost the same *nc*-Si size (~4.5 nm). In general, the dielectric functions of bulk crystalline silicon show main peaks at the transition energies E_1 (~3.4 eV) and E_2 (~4.3 eV) as its critical points. As for the case of *nc*-Si formed after high-temperature annealing, the dielectric functions show a slight blueshift in the main transition energy E_1 (~3.6 eV) position, and a slight redshift in the E_2 (~4.0 eV) position. However, in the case of the as-implanted (i.e., nonannealing) sample, the dielectric functions of *nc*-Si show only a single peak in the experimental photon-energy range, possibly because of larger broadenings of E_1 and E_2 band gaps due to a large change of surface area to volume ratio when the size of *nc*-Si is close to 3 nm.

On the other hand, the static dielectric constant ($\varepsilon_{\text{static}}^{\text{exp}}$) of *nc*-Si is obtained by setting the photon energy to zero in the FB model, and the result is given in Table I. Thanks to the extensive studies on the nanostructured silicon, the fact that the suppression of the dielectric constant becomes significant when the nanocrystal size approaches the nanometric range is, nowadays, unquestionable. However, the origin of the reduction in dielectric constant with decreasing size is still under debate. Among the different mechanisms proposed for dielectric suppression of nanoscale materials, most are related to: (i) opening of the band gap, which lowers the polarizability, and (ii) the breaking of polarizable bonds at the surface. Nevertheless, in the present study, the static dielectric constant of *nc*-Si is found to be significantly suppressed as compared to that of bulk crystalline silicon, as shown in Table I. Taking the screening effect by the medium into account, the static dielectric constant of the *nc*-Si as a function of the nanocrystal size could be expressed as follows:[9]

$$\varepsilon_{\text{static}}(D) = 1 + \frac{\varepsilon_{\text{static}}(\infty) - 1}{1 + \left(\dfrac{1.38}{D}\right)^{1.37}}, \tag{2}$$

where $\varepsilon_{\text{static}}(\infty)$ is the static dielectric constant of bulk crystalline silicon and D is the diameter of *nc*-Si with the unit of nm. The static dielectric constant calculated with Eq. (2) is also presented in Table I. It can be seen in the table that there is a good agreement between the values ($\varepsilon_{\text{static}}^{\text{cal}}$) calculated from Eq. (2) and the extracted values ($\varepsilon_{\text{static}}^{\text{exp}}$) from the SE analysis.

In conclusion, we have investigated the thermal annealing effect on the dielectric functions and band gap of silicon nanocrystals embedded in a SiO_2 matrix by spectroscopic ellipsometry. In the SE analysis, a multilayer optical model that takes into account the *nc*-Si distributions in the SiO_2 film, the Maxwell-Garnett effective medium approximation, and the four-term Forouhi-Bloomer optical dispersion relation are used. The dielectric functions of *nc*-Si for different annealing durations show a significant suppression as compared to bulk crystalline silicon, which is attributed to the quantum size effect. The *nc*-Si of the as-implanted (i.e., nonannealing) sample presents only one peak in the dielectric spectra, while the annealed ones have two critical points in the range of 1–5 eV. The *nc*-Si for various annealing durations shows a large band-gap expansion of ~0.6 eV, which is in good agreement with the theoretical calculation based on quantum confinement. The band gap of the *nc*-Si for the nonannealing condition (i.e., as implanted) is 1.78 eV while it is 1.72 eV for the annealing at 1000 °C for 100 min. The slight decrease in the band gap is attributed to the slight increase in the *nc*-Si size with annealing.

This work has been financially supported by the Ministry of Education Singapore under Project No. ARC 1/04.

[1] L. T. Canham, Appl. Phys. Lett. **57**, 1046 (1990).
[2] M. A. Tichler, R. T. Collins, J. H. Stathis, and J. C. Tsang, Appl. Phys. Lett. **60**, 639 (1992).
[3] P. Mutti, G. Ghislotti, S. Bertoni, L. Bonoldi, G. F. Cerofolini, L. Meda, E. Grilli, and M. Guzzi, Appl. Phys. Lett. **66**, 851 (1994).
[4] K. S. Zhuravlev, A. M. Gilinsky, and A. Yu. Kobitsky, Appl. Phys. Lett. **73**, 2962 (1998).
[5] X. L. Wu, S. J. Xiong, G. G. Siu, G. S. Huang, Y. F. Mei, Z. Y. Zhang, S. S. Deng, and C. Tan, Phys. Rev. Lett. **91**, 157402 (2003).
[6] P. J. Walters, G. I. Bourianoff, and H. A. Atwater, Nat. Mater. **4**, 143 (2005).
[7] J. Linnros, Nat. Mater. **4**, 117 (2005).
[8] A. Irrera, D. Pacifici, M. Miritello, G. Franzo, F. Priolo, F. Iacona, D. Sanfilippo, G. D. Stefano, and P. G. Fallica, Physica E (Amsterdam) **16**, 395 (2003).
[9] L. W. Wang and A. Zunger, Phys. Rev. Lett. **73**, 1039 (1994).
[10] C. Delerue, G. Allan, and M. Lannoo, Phys. Rev. B **48**, 11024 (1993).
[11] S. Ogut, J. R. Chelikowsky, and S. G. Louie, Phys. Rev. Lett. **79**, 1770 (1997).
[12] I. Vasiliev, S. Ogut, and J. R. Chelikowsky, Phys. Rev. Lett. **86**, 1813 (2001).
[13] H.-Ch. Weissker, J. Furthmüller and F. Bechstedt, Phys. Rev. B **65**, 155327 (2002).
[14] A. R. Forouhi and I. Bloomer, Phys. Rev. B **38**, 1865 (1988).
[15] T. P. Chen, Y. Liu, M. S. Tse, O. K. Tan, P. F. Ho, and K. Y. Liu, Phys. Rev. B **68**, 153301 (2003).
[16] G. Garrido, M. Lopez, O. Gonzalez, A. P. Rodriguez, J. R. Morante, and C. Bonafos, Appl. Phys. Lett. **77**, 3143 (2000).
[17] *Guide to Using* WVASE32TM (WexTech Systems, Inc., Madison Avenue, New York).

Downloaded 19 Apr 2007 to 147.8.143.135. Redistribution subject to AIP license or copyright, see http://apl.aip.org/apl/copyright.jsp